Reference interferometer using a semiconductor laser/LED reference source in a cryogenic Fourier-transform spectrometer

Anthony J. Martino and Donald M. Cornwell

Lasers and Electro-Optics Branch, Code 554, NASA Goddard Space Flight Center, Greenbelt, MD 20771

ABSTRACT

A combination of a single mode AlGaAs laser diode and a broadband LED was used in a Michelson interferometer to provide reference signals in a Fourier transform spectrometer, the Composite Infrared Spectrometer, on the Cassini mission to Saturn. The narrowband light from the laser produced continuous fringes throughout the travel of the interferometer, which were used to control the velocity of the scan mechanism and to trigger data sampling. The broadband light from the LED produced a burst of fringes at zero path difference, which was used as a fixed position reference. The system, including the sources, the interferometer, and the detectors, was designed to work both at room temperature and at the instrument operating temperature of 170 Kelvin. One major challenge that was overcome was preservation, from room temperature to 170 K, of alignment sufficient for high modulation of fringes from the broadband source. Another was the shift of the source spectra about 30 nm toward shorter wavelengths upon cooldown.

Keywords: Fourier transform spectrometer, laser diode, LED, Cassini, CIRS, reference interferometer

1. INTRODUCTION

The Composite Infrared Spectrometer[1,2] (CIRS) for the Cassini mission to Saturn is a Fourier transform infrared spectrometer that contains three Michelson-type interferometers. One is used for spectral measurements in the mid-infrared (MIR) band of 7 to 17 μm; another is used in the far-infrared (FIR) band of 17 to 1000 μm. The moving elements of these two interferometers are mounted on a common scan mechanism[3].

The third interferometer, called the reference interferometer (RI), is the subject of this paper. In a Fourier transform spectrometer, it is essential to have precise knowledge of the position of the moving element as it moves. In CIRS, the reference interferometer provides this information. It is also a Michelson-type interferometer, with one of its arms terminated on the same scan mechanism as the MIR and FIR interferometers. The signals produced by the RI are used in two ways: as feedback to the circuits that control motion of the scan mechanism, and as a trigger signal for the sampling of data from the detectors in the MIR and FIR interferometers.

2. DESIGN OVERVIEW

The RI is a Michelson interferometer with cube-corner retroreflectors at the ends of its arms. (See Figure 1). Two light sources, a single-frequency laser diode and a wide-spectrum LED, emit light into the RI. Their outputs are combined with a polarizing beamsplitter and collimated, and a quarter-wave plate is used for isolation.

The collimated beams are sent into the interferometer, where they are split by a nonpolarizing beamsplitter. Both arms are terminated by retroreflectors; the moving retroreflector is actually the central portion of the element that is used in the MIR interferometer. The other retroreflector is fixed to the optical bench.

The output beams from the interferometer are split, filtered, and focused onto pinholes to separate the laser light from the LED light. Behind each pinhole is a photodetector.

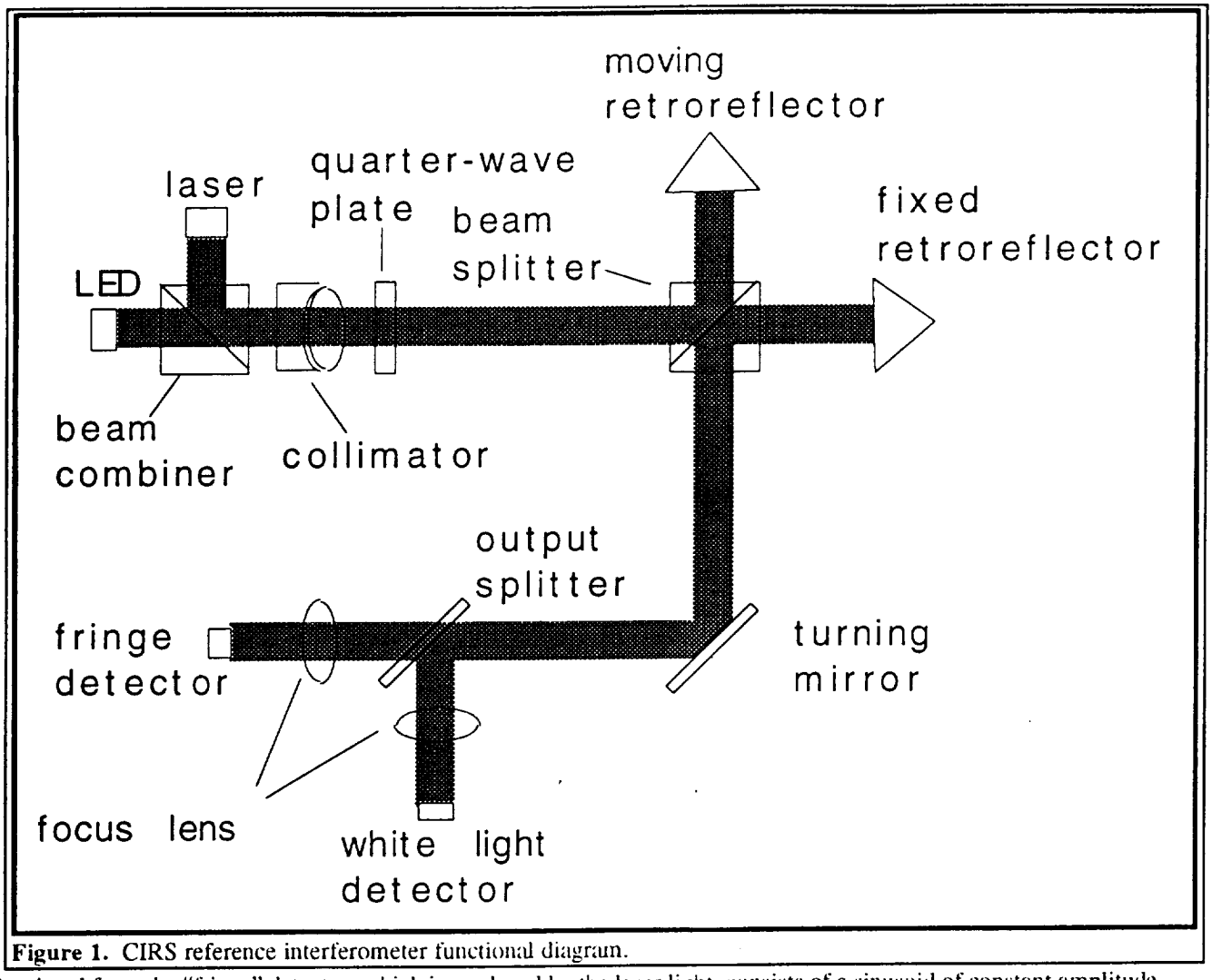

Figure 1. CIRS reference interferometer functional diagram.

The signal from the "fringe" detector, which is produced by the laser light, consists of a sinusoid of constant amplitude, which goes through one cycle as the scan mechanism moves half the wavelength of the laser light. The reference interferometer electronics (RIE) detects the positive and negative zero-crossings of this signal and converts them to a digital pulse train. The scan mechanism electronics lock this pulse train to a fixed frequency, causing the scan mechanism to move at a constant speed.

The signal from the "white light" detector consists of a flat line most of the time, with a burst occurring as the RI passes through zero path difference (ZPD). The burst consists of about 12 sinusoidal cycles under a roughly Gaussian envelope. The period of the sinusoid is half the mean wavelength of the LED, and the highest peak is at ZPD. When the RIE detects the highest peak, it begins to send the fringe pulse train to the front end electronics, where it is used to trigger sampling of data from the scientific focal planes.

3. SOURCES

In the previous instruments[4,5,6] for long-term space missions, on which the original design for CIRS was based, neon gas discharge lamps were used as reference sources. The neon spectrum contains a few discrete, easily separable lines, any one of which can be used to create a continuous series of fringes over a few millimeters of path length difference. It also contains a broadband "continuum" that can be used to create "white light" fringes.

In a few other spaceborne Fourier transform instruments, in which power and thermal dissipation were less of an issue than in CIRS, HeNe gas lasers were used as reference sources. In most planned future instruments, diode or solid-state lasers are used (in some cases, as a result of the work reported here). A review of past and planned spaceborne Fourier transform spectrometers has been published by Persky[7].

During the development of CIRS, it was discovered that neon lamps were not up to the increased demands presented by CIRS. Problems were encountered in several areas: lifetime verification, signal strength, and behavior of the lamps at cryogenic temperatures.

The nominal lifetimes of commercially-available neon indicator lamps, particularly when operated at DC, were significantly less that the minimum requirement of 26,000 hours for CIRS. Therefore, in the baseline design, two lamps were provided. The lamps would be run at a reduced current in order to extend their lifetime. A series of tests was conducted on several lamp models to verify the relation between drive current and lifetime, and to verify by accelerated test that the lamps would meet the required lifetime. The test failed to verify the relation between current and lifetime given in the manufacturers' data sheets; in fact it did not yield any usable relation. Therefore, since the duration of the test was only slightly more than 1000 hours, it was inconclusive with respect to overall the lifetime requirement.

The issue of signal strength was more immediately apparent. The light emission from the neon lamps was spread through a glow discharge region approximately 1mm x 1 mm. Using a field of view of 330 μm on the lamp, it was possible to get an adequate signal-to-noise ratio in fringe channel over the entire range of travel when the interferometer was perfectly aligned. With the same field of view, it was also possible to get an adequate signal-to-noise ratio in the white-light channel at ZPD under the same conditions. However, sensitivity of signal modulation to misalignment increases as the field of view is enlarged.[8,9] When the interferometer was cooled from room temperature to its required operating temperature of 170 K, it suffered sufficient misalignment that the resulting signals were useless. While the optical power incident on the detectors decreased only slightly, fringe modulation degraded so badly that the fringe pattern was often lost in the detector noise.

An even more serious problem also occurred with the transition to cryogenic temperatures. This was the tendency of the plasma discharge within the lamps to move as a function of temperature, and eventually to become unstable. "Flickering", that is, rapid motion of the discharge between two positions, occurred in almost every lamp below about 220 K. While the spatially integrated output of the lamp remained relatively constant, the signal from a detector looking at a fixed field of view showed very large jumps as the discharge switched position. Fringe and white light signals produced under these conditions were not usable, even if their signal-to-noise ratios were otherwise acceptable.

As a result of these problems and uncertainties, the neon lamp design was abandoned in favor of a semiconductor diode light source. This source consisted of a laser diode and a LED, combined optically. Both devices emitted far more light than the neon lamp from a smaller emitting area. This allowed a very strong signal to be collected from a much smaller field of view, reducing the sensitivity to alignment. In addition, both had proven lifetimes, and we were able to show that they had no objectionable behavior at 170 K.

The laser chosen for this instrument is a modified version of the SDL 5601[10]. It is mounted to an aluminum structure with a thin Delrin bushing to provide electrical insulation. A single-frequency Fabry-Perot laser diode, it emits at about 810 nm at room temperature and 783 nm at 170 K. Highly linearly polarized light is emitted from an area approximately 1x3 μm into a cone approximately 10° x 30°. Each device has two emitting areas, spaced about 14 μm apart, that can be controlled independently. Between mode hops, the laser exhibits a temperature coefficient of 0.08 nm/K. Since the laser wavelength stability requirement is 1 part in 10^5 over a 2-minute time interval, it is necessary to stabilize the temperature to prevent excursions of more than 0.01 K in that time. The structure in which the RI is mounted is controlled to ± 0.1°C in 24 hours, and its thermal inertia is sufficient to prevent extremely rapid temperature changes.

The LED that is used as a "white light" source is the Opto-Diode OD880[11]. Light is emitted from the edges of the diode into a well in the bottom of the case; it is the diffuse surface of the well that serves as the effective light source for the interferometer. At room temperature, it emits in an approximately 80 nm wide bandwidth centered around 890 nm. At 170 K, the bandwidth narrows somewhat, and the total power approximately doubles for a given drive current (see Figure 2).

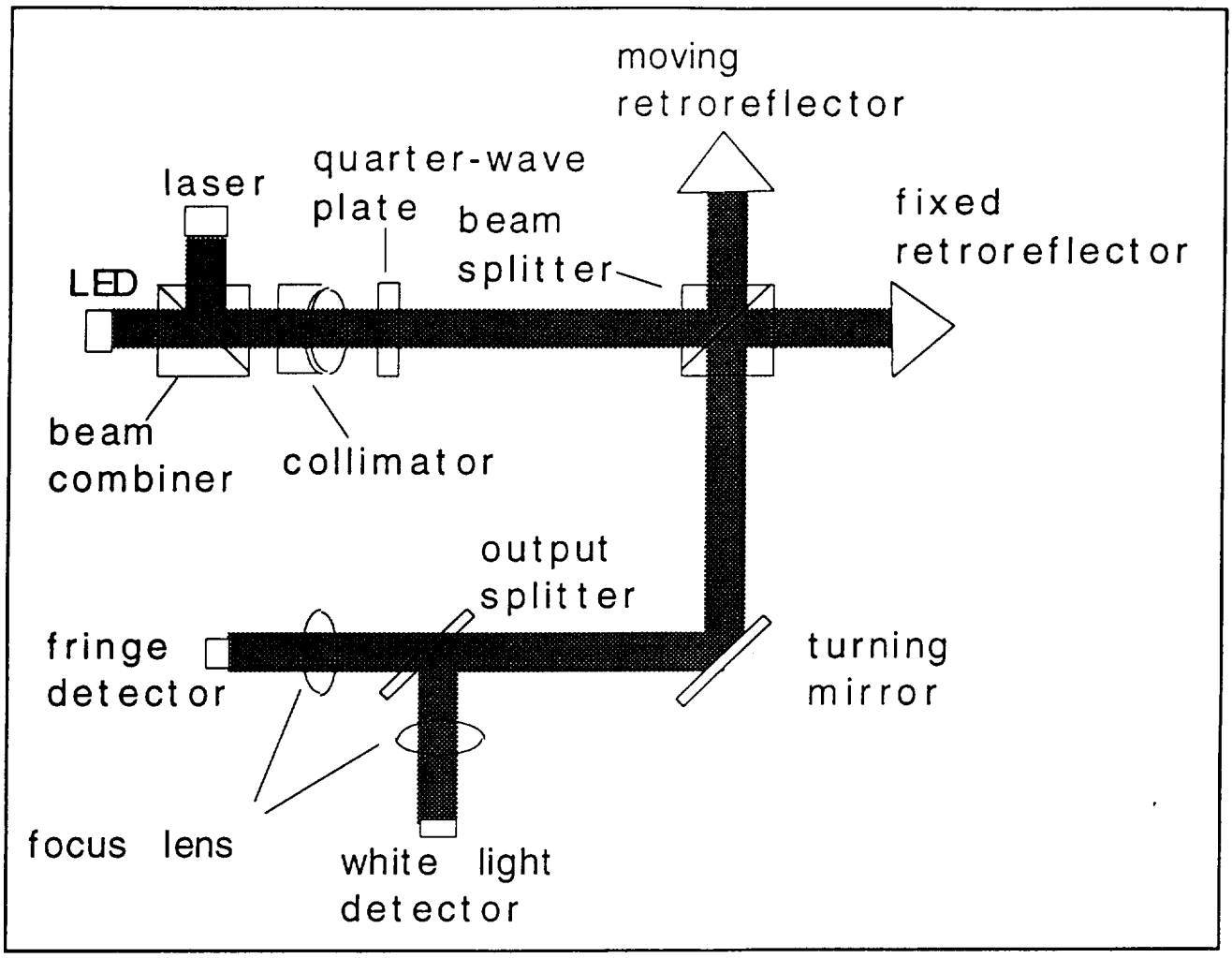

Figure 1. CIRS reference interferometer functional diagram.

The signal from the "fringe" detector, which is produced by the laser light, consists of a sinusoid of constant amplitude, which goes through one cycle as the scan mechanism moves half the wavelength of the laser light. The reference interferometer electronics (RIE) detects the positive and negative zero-crossings of this signal and converts them to a digital pulse train. The scan mechanism electronics lock this pulse train to a fixed frequency, causing the scan mechanism to move at a constant speed.

The signal from the "white light" detector consists of a flat line most of the time, with a burst occurring as the RI passes through zero path difference (ZPD). The burst consists of about 12 sinusoidal cycles under a roughly Gaussian envelope. The period of the sinusoid is half the mean wavelength of the LED, and the highest peak is at ZPD. When the RIE detects the highest peak, it begins to send the fringe pulse train to the front end electronics, where it is used to trigger sampling of data from the scientific focal planes.

3. SOURCES

In the previous instruments[4,5,6] for long-term space missions, on which the original design for CIRS was based, neon gas discharge lamps were used as reference sources. The neon spectrum contains a few discrete, easily separable lines, any one of which can be used to create a continuous series of fringes over a few millimeters of path length difference. It also contains a broadband "continuum" that can be used to create "white light" fringes.

In a few other spaceborne Fourier transform instruments, in which power and thermal dissipation were less of an issue than in CIRS, HeNe gas lasers were used as reference sources. In most planned future instruments, diode or solid-state lasers are used (in some cases, as a result of the work reported here). A review of past and planned spaceborne Fourier transform spectrometers has been published by Persky[7].

During the development of CIRS, it was discovered that neon lamps were not up to the increased demands presented by CIRS. Problems were encountered in several areas: lifetime verification, signal strength, and behavior of the lamps at cryogenic temperatures.

The nominal lifetimes of commercially-available neon indicator lamps, particularly when operated at DC, were significantly less that the minimum requirement of 26,000 hours for CIRS. Therefore, in the baseline design, two lamps were provided. The lamps would be run at a reduced current in order to extend their lifetime. A series of tests was conducted on several lamp models to verify the relation between drive current and lifetime, and to verify by accelerated test that the lamps would meet the required lifetime. The test failed to verify the relation between current and lifetime given in the manufacturers' data sheets; in fact it did not yield any usable relation. Therefore, since the duration of the test was only slightly more than 1000 hours, it was inconclusive with respect to overall the lifetime requirement.

The issue of signal strength was more immediately apparent. The light emission from the neon lamps was spread through a glow discharge region approximately 1mm x 1 mm. Using a field of view of 330 μm on the lamp, it was possible to get an adequate signal-to-noise ratio in fringe channel over the entire range of travel when the interferometer was perfectly aligned. With the same field of view, it was also possible to get an adequate signal-to-noise ratio in the white-light channel at ZPD under the same conditions. However, sensitivity of signal modulation to misalignment increases as the field of view is enlarged.[8,9] When the interferometer was cooled from room temperature to its required operating temperature of 170 K, it suffered sufficient misalignment that the resulting signals were useless. While the optical power incident on the detectors decreased only slightly, fringe modulation degraded so badly that the fringe pattern was often lost in the detector noise.

An even more serious problem also occurred with the transition to cryogenic temperatures. This was the tendency of the plasma discharge within the lamps to move as a function of temperature, and eventually to become unstable. "Flickering", that is, rapid motion of the discharge between two positions, occurred in almost every lamp below about 220 K. While the spatially integrated output of the lamp remained relatively constant, the signal from a detector looking at a fixed field of view showed very large jumps as the discharge switched position. Fringe and white light signals produced under these conditions were not usable, even if their signal-to-noise ratios were otherwise acceptable.

As a result of these problems and uncertainties, the neon lamp design was abandoned in favor of a semiconductor diode light source. This source consisted of a laser diode and a LED, combined optically. Both devices emitted far more light than the neon lamp from a smaller emitting area. This allowed a very strong signal to be collected from a much smaller field of view, reducing the sensitivity to alignment. In addition, both had proven lifetimes, and we were able to show that they had no objectionable behavior at 170 K.

The laser chosen for this instrument is a modified version of the SDL 5601[10]. It is mounted to an aluminum structure with a thin Delrin bushing to provide electrical insulation. A single-frequency Fabry-Perot laser diode, it emits at about 810 nm at room temperature and 783 nm at 170 K. Highly linearly polarized light is emitted from an area approximately 1x3 μm into a cone approximately 10° x 30°. Each device has two emitting areas, spaced about 14 μm apart, that can be controlled independently. Between mode hops, the laser exhibits a temperature coefficient of 0.08 nm/K. Since the laser wavelength stability requirement is 1 part in 10^5 over a 2-minute time interval, it is necessary to stabilize the temperature to prevent excursions of more than 0.01 K in that time. The structure in which the RI is mounted is controlled to ± 0.1°C in 24 hours, and its thermal inertia is sufficient to prevent extremely rapid temperature changes.

The LED that is used as a "white light" source is the Opto-Diode OD880[11]. Light is emitted from the edges of the diode into a well in the bottom of the case; it is the diffuse surface of the well that serves as the effective light source for the interferometer. At room temperature, it emits in an approximately 80 nm wide bandwidth centered around 890 nm. At 170 K, the bandwidth narrows somewhat, and the total power approximately doubles for a given drive current (see Figure 2).

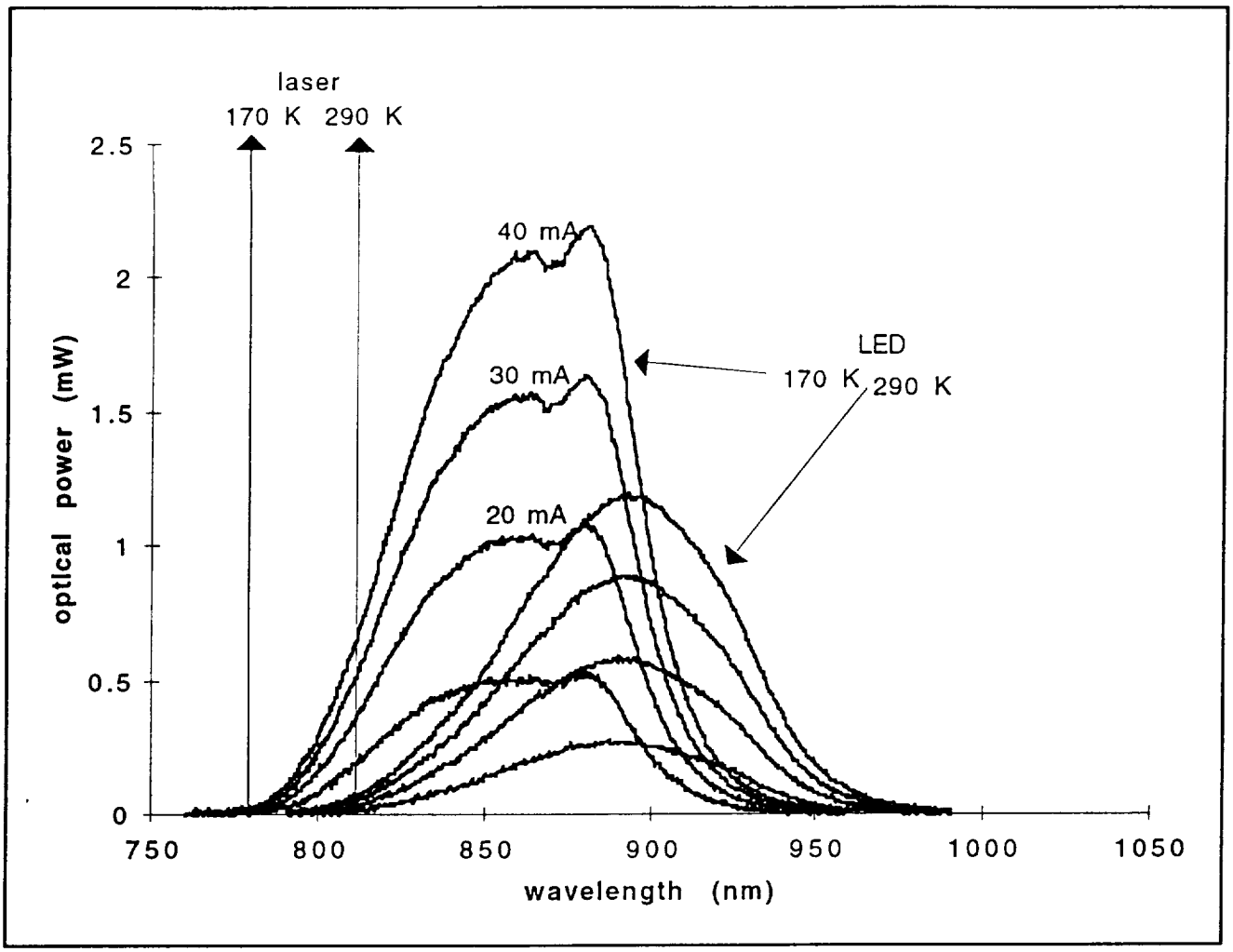

Figure 2. Dependence of source spectra on temperature and drive current

4. OPTICS

The optics can be divided into three sections: the source optics, which form the beams; the interferometer optics, which modulate the beams; and the receiver optics, which separate the laser and LED beams and focus them onto their respective detectors.

The lenses and beam splitters and combiners are all made from two radiation-resistant glass types: Schott BK7-G25 and LF5-G15. The instrument is required to withstand up to 100 krad, mostly from high-energy protons.

4.1. Source optics

The LED is placed with its center on the optical axis of the interferometer. Half of its randomly-polarized light is transmitted by the polarizing beam combiner. It is collimated by the 28 mm focal length doublet into a 9 mm diameter beam, which is sent into the interferometer.

The difference in power output between the laser and the LED is so large that spectral filtering alone would not be sufficient to separate the two beams at the output of the interferometer. In addition, the retroreflectors in the interferometer would send a large portion of the laser light back to its source, creating severe instability in the frequency and power output of the laser. These problems were alleviated by putting the LED on axis and the laser off axis and introducing an input aperture into the laser's optical path. (See Figure 3.) The spatial separation between the laser and the LED is repeated in the image plane at the output of the system, so the "white light" detector sees only scattered light from the laser. The laser input aperture

reduces the amount of laser light that enters the interferometer. Also, it causes all of the laser light to hit the retroreflectors on one side of center. The returned beam is on the other side of center, and therefore misses the aperture and does not hit the laser.

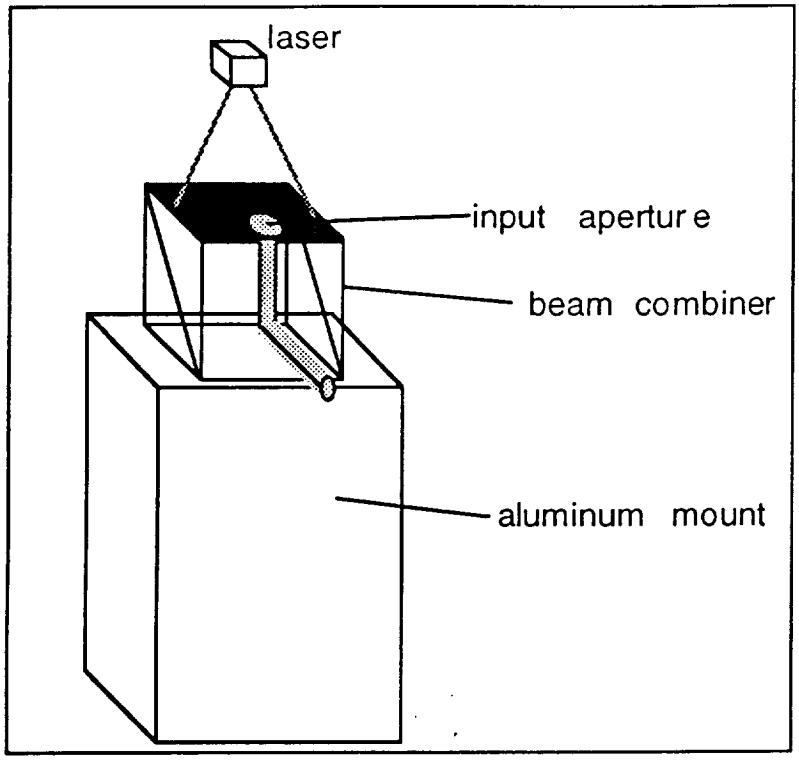

Figure 3. Laser input optics

The laser input aperture and the beam combiner mount are made of aluminum. They are bonded to the glass beam combiner with RTV566[12], a silicone rubber adhesive, after preparing the surfaces with SS4155 primer. While the resulting bond is strong enough to withstand the vibration of launch, it is still compliant enough to prevent breakage due to differential contraction between the glass and aluminum as the instrument is cooled from room temperature to 170 K.

While the input aperture effectively prevents the retroreflectors from causing feedback into the laser, it does nothing to prevent feedback from flat surfaces perpendicular to the beam. While reflections from these surfaces are minimized by antireflection coatings, an additional measure of protection is obtained by using a crystalline quartz quarter-wave plate after the collimator. The laser is oriented so that its light is reflected by the polarizing beam combiner. The quarter-wave plate has its axis at 45° to the polarization of the incident laser light. Light that is reflected back from perpendicular surfaces in the interferometer has its polarization rotated 90° after the second pass through the quarter-wave plate. Rather than being reflected back into the laser by the beam combiner, it is transmitted harmlessly onto the LED.

4.2. Interferometer optics

The laser and LED beams follow a common path through the interferometer. They are split by a nonpolarizing cube beamsplitter. The reflected beam is returned from the moving retroreflector, and the transmitted beam is returned from the fixed retroreflector. The returned beams are recombined at the beamsplitter, then directed by a fold mirror to the receiver.

Preservation of alignment between the beamsplitter and the two retroreflectors during the transition from room temperature to 170 K is vital to the performance of the interferometer. In a Michelson interferometer that uses cube corner retroreflectors, the critical alignment is shear between the two beams. This can be affected by tilt of the beamsplitter and translation of the cube corners.

The cube beamsplitter was fabricated with a cylindrical extension on the face toward the fold mirror. The extension is inserted in one end of a cylindrical portion of the interferometer structure, and the fold mirror is inserted in the other end. (See Figure 4.) RTV 566 is injected through small holes in the aluminum cylinder to hold the optics in place. In earlier versions, the cylinder was a separate piece, bonded with RTV 566 to the rest of the structure. This arrangement did not maintain alignment well enough on cooldown. In the flight unit, the entire structure ("interferometer housing") shown in Figure 4 is a single piece of aluminum, which is bolted into the CIRS optical bench. The source and receiver packages are bolted onto the interferometer housing.

The moving and fixed retroreflectors are glass hollow cube corners, made at Goddard Space Flight Center[13,14]. The moving reflector is shared with the MIR interferometer and is mounted on the scan mechanism. The MIR interferometer uses the

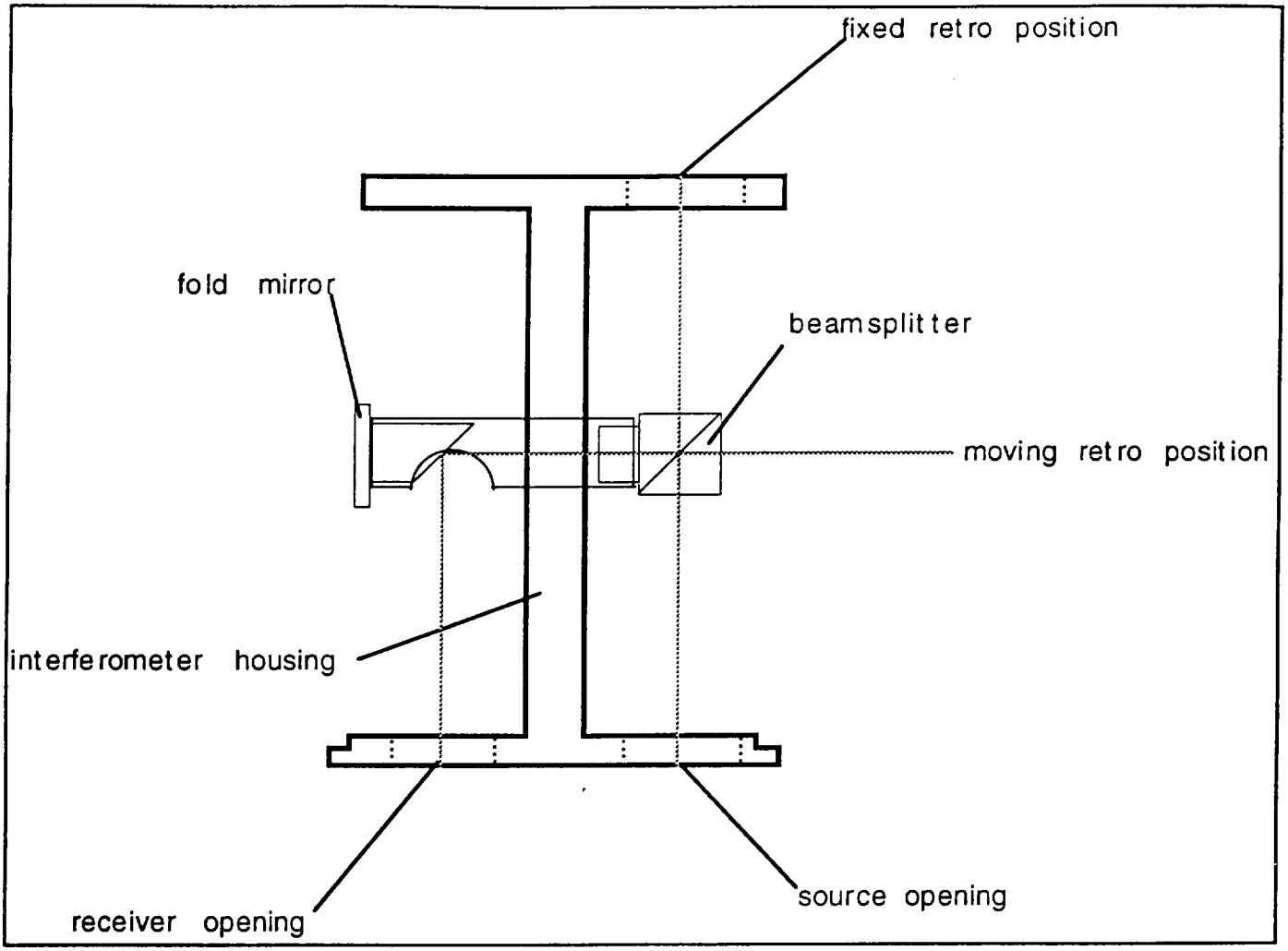

Figure 4. Interferometer structure

outer portion of the reflector, while the RI, which is located in the shadow of the telescope secondary mirror, uses the central portion. The fixed reflector is mounted on the optical bench.

The fold mirror was diamond-turned at 45° to the axis of an aluminum cylinder at Marshall Space Flight Center, then coated with gold at Goddard.

4.3. Receiver optics

The receiver consists of two channels. The "fringe" signal is detected in one channel, and the "white light" signal is detected in the other. Light that comes from the interferometer is divided between the two channels by a neutral beamsplitter, which reflects 90% of the light into the "white light" channel and transmits 10% into the "fringe" channel.

In each channel, the desired signal is separated from the other signal, and from stray light, by spectral and spatial filtering. A 28 mm focal length singlet lens focuses the collimated beams, forming a unit-magnification image of the sources at its focal plane. The "fringe" lens is coated with a multi-layer interference coating that is designed to pass the laser wavelength but block the LED spectrum at 170 K. The "white light" focus lens has a coating that does the opposite. Because of the close spacing between the laser and LED wavelengths (see Figure 2), it is not possible to design a coating that cleanly separates the two spectra at both room temperature and 170 K, so some crosstalk is unavoidable at room temperature.

A 150 μm diameter circular field stop is located in the focal plane of each lens. The "fringe" field stop, which is centered on the image of the laser, serves mostly to block stray light, since the image of the laser is smaller than the aperture diameter. The "white light" field stop, which is centered on the image of the LED, actually limits the area of the image that is "seen" by the detector. This is necessary to limit the sensitivity of the signal to shear.

Because of the large difference in power between the laser and LED, the blocking performance of the "white light" interference filter is only good enough to prevent crosstalk from the peripheral regions of the laser beam. However, the laser and the LED are offset by more than the field size in the source plane, so the direct laser beam is blocked by the field stop in the "white light" focal plane.

5. DETECTORS

Photodetectors are located directly behind the field stops in both receiver channels. Both detectors are EG&G SGD100 silicon PIN photodiodes[15]. These detectors have 2.5 mm diameter active areas, so they are oversized with respect to the cone of light coming through the field stop. This makes them relatively insensitive to alignment.

Each photodiode is followed by a transimpedance amplifier. The gains of the amplifiers are set to put the output signals between 0 and 10 Volts for the range of optical inputs.

6. PERFORMANCE

Figures 9 through 12 show examples of the fringe and white light signals produced by the RI hardware after its installation into the Cassini CIRS instrument. The data for figures 9 and 10 were measured with the instrument cooled to 170 K in a thermal vacuum chamber. The data for figures 11 and 12 were measured with the instrument at room temperature in air.

In general, the performance of the interferometer is better at its inteded operating temperature of 170 K than at room temperature. Reasons for this include greater efficiency of the light sources and better spectral properties of the laser when cold, and better separation of the channels as the spectra of the light sources shifts to the wavelengths for which the interference filters were designed.

The greater efficiency of the laser and LED means that a stronger signal is obtained for a given drive current. This effect is most evident in the white light signals. Both sets shown here were measured at the same drive current; the height in the cold case is twice what it is in the warm case. For the fringe signals, this is less evident, because it was necessary to run the laser at different drive currents depending on temperature. Typically, the laser drive current is reduced by about a factor of 2 between room temperature and 170 K.

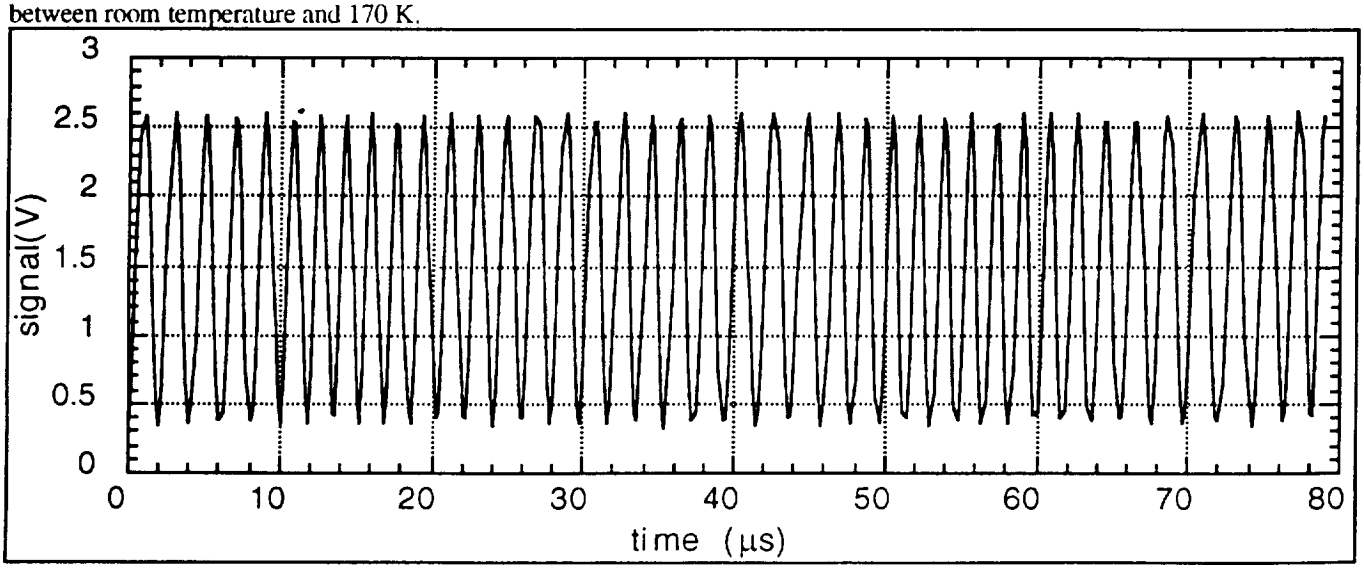

Figure 9. Fringe signal at instrument operating temperature of 170 K.

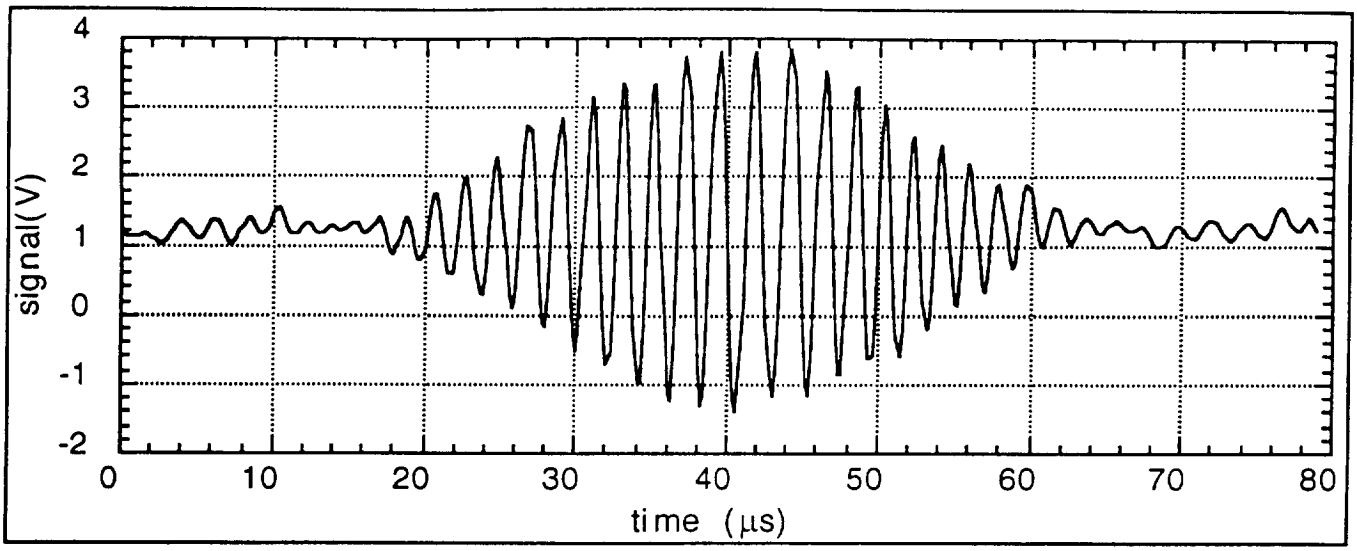

Figure 10. White light signal at instrument operating temperature of 170 K.

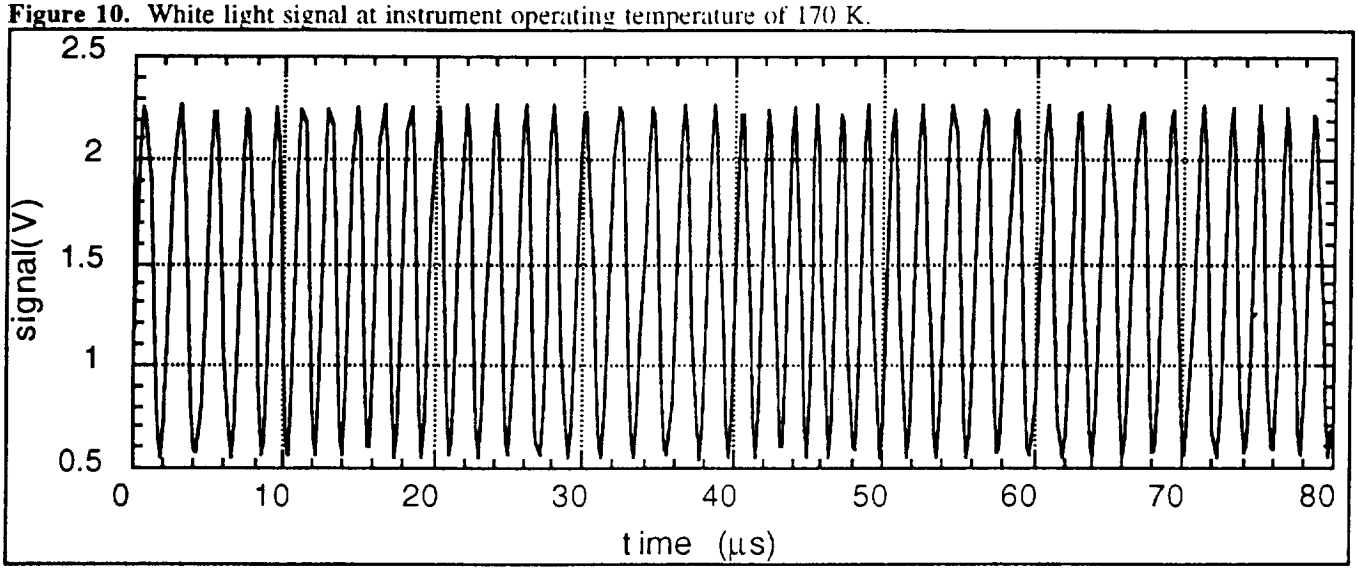

Figure 11. Fringe signal at room temperature.

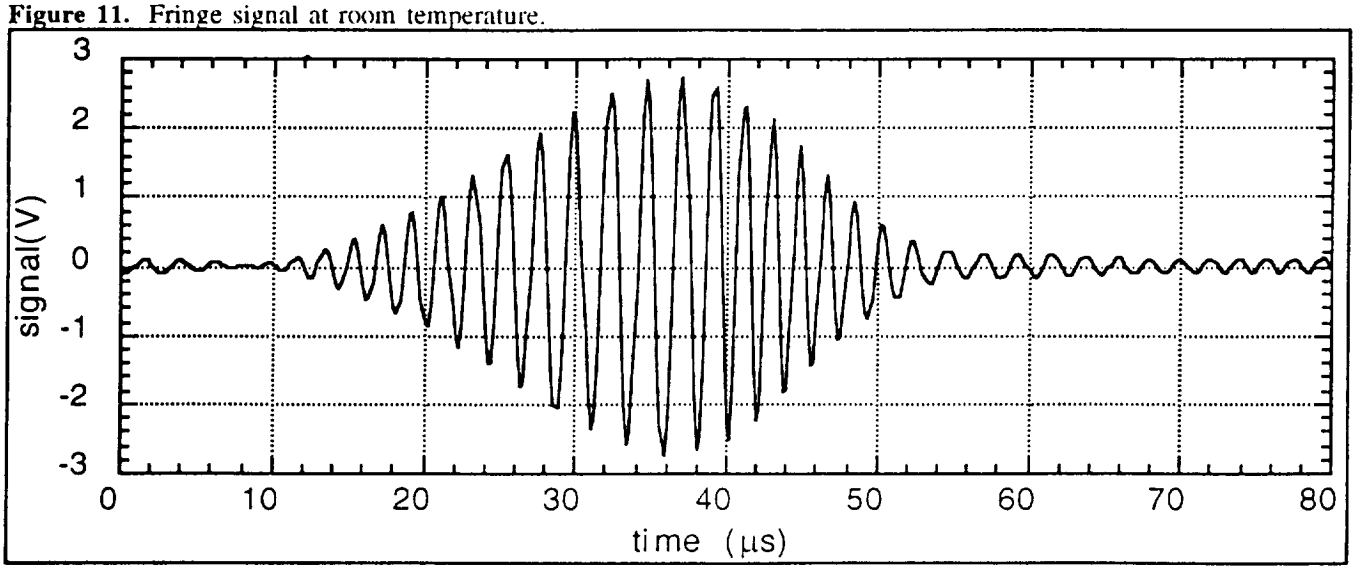

Figure 12. White light signal at room temperature.

At 170 K, the laser diode operates at a single frequency over a very wide range of drive currents. While the lasers used in the engineering models of the CIRS RI are almost this good at room temperature as well, the batch that was produced for flight was found to be single-frequency only within a few very narrow ranges of drive current. Since the instrument temperature is not under control at room temperature, the laser tends to drift. Consequently, it usually runs multimode. This produces a fringe height that varies over the length of the scan, due to beating between the two frequencies. While such behavior would not be acceptable at the operating temperature, it is sufficient for the operations that are necessary at room temperature.

As mentioned before, the separation between the laser and LED spectra is about the same as their common shift between room temperature and 170 K, so it is not possible to separate them cleanly at both temperatures with a fixed filter. Comparison of the warm and cold white light signals shows evidence of this. While the signal away from the white light fringes shows only noise in the cold case, it clearly shows leakage of the fringe signal in the warm case.

The CIRS instrument, including the reference interferometer, was launched aboard the Cassini spacecraft in October, 1997 and is now on its way to Saturn. Telemetry signals have been received from CIRS RI on several occasions since then, and all are within their nominal range. All indications are that it is working properly, giving the same performance as before launch.

7. REFERENCES

1. V. Kunde *et. al.*, "Cassini infrared Fourier spectroscopic investigation," *Proc. SPIE* **2803**, pp. 162-177, 1996.
2. P. W. Maymon *et al.*, "Optical design of the composite infrared spectrometer (CIRS) for the Cassini mission," *Proc. SPIE* **1945**, pp. 100-111, 1993.
3. C. F. Hakun and K. A. Blumenstock, "A cryogenic scan mechanism for use in Fourier transform spectrometers," in *NASA Johnson Space Flight Center 29th Aerospace Mechanisms Symposium*, pp. 316-333, 1995.
4. R. Hanel *et al.*, "Infrared spectrometer for Voyager," *Appl. Opt.* **19**, pp. 1391-1400, 1980.
5. R. Hanel *et al.*, "Mariner 9 Michelson Interferometer," *Appl. Opt.* **11**, pp. 2625-2634, 1972.
6. R. Hanel *et al.*, "The Nimbus III Michelson Interferometer," *Appl. Opt.* **9**, pp. 1767-1774, 1970.
7. M. J. Persky, "A review of spaceborne infrared Fourier transform spectrometers for remote sensing," *Rev. Sci. Instrum.* **66**, pp. 4763-4796, 1995.
8. M. V. R. K. Murty, "Some more aspects of the Michelson interferometer with cube corners,"*J. Opt. Soc. Am.* **50**, pp. 7-10, 1960.
9. A. J. Martino and J. G. Hagopian, "Effects of shear, defocus, and wavefront error on the theoretical performance of the composite infrared spectrometer for Cassini," *Proc. SPIE* **3435**, in press, 1998.
10. SDL, Inc., 80 Rose Orchard Way, San Jose, CA 95134.
11. Opto-Diode Corp., 750 Mitchell Road, Newbury Park, CA 91320.
12. GE Silicones, 260 Hudson River Road, Waterford, NY 12188.
13. J. J. Lyons and P. A. Hayes, "High-optical-quality cryogenic hollow retroreflectors," *Proc. SPIE* **2540**, pp. 94-100, 1995.
14. P. A. Hayes, D. E. Jennings, and J. J. Lyons, "Development and testing of the Composite Infrared Spectrometer (CIRS) retroreflectors," *Proc. SPIE* **2227**, pp. 37-43, 1994.
15. EG&G Canada, 22001 Dumberry Road, Vaudreuil, Quebec, Canada J7V 8P7.